arXiv:2103.07130v2 [physics.atom-ph] 1 Dec 2021

Magnetic Feshbach resonances in collisions of ^{23}Na^{40}K with ^{40}K

Xin-Yao Wang[1,2,4,5,6],* Matthew D. Frye[3,*],† Zhen Su[2,4,5], Jin Cao[2,4,5], Lan Liu[2,4,5], De-Chao Zhang[2,4,5], Huan Yang[2,4,5], Jeremy M. Hutson[3],‡ Bo Zhao[2,4,5],§ Chun-Li Bai[1,2,6],¶ and Jian-Wei Pan[2,4,5]**

[1] *Beijing National Laboratory for Molecular Sciences, Key Laboratory of Molecular Nanostructure and Nanotechnology, CAS Research/Education Center for Excellence in Molecular Sciences, Institute of Chemistry, Chinese Academy of Sciences, Beijing 100190, China*

[2] *Hefei National Laboratory for Physical Sciences at the Microscale and Department of Modern Physics, University of Science and Technology of China, Hefei, Anhui 230026, China*

[3] *Joint Quantum Centre (JQC) Durham-Newcastle, Department of Chemistry, Durham University, South Road, Durham DH1 3LE, United Kingdom*

[4] *Shanghai Branch, CAS Center for Excellence and Synergetic Innovation Center in Quantum Information and Quantum Physics, University of Science and Technology of China, Shanghai 201315, China*

[5] *Shanghai Research Center for Quantum Sciences, Shanghai 201315, China and*

[6] *University of Chinese Academy of Sciences, Beijing 100049, China*

(Dated: December 2, 2021)

We present measurements of more than 80 magnetic Feshbach resonances in collisions of ultracold ^{23}Na^{40}K with ^{40}K. We assign quantum numbers to a group of low-field resonances and show that they are probably due to long-range states of the triatomic complex in which the quantum numbers of the separated atom and molecule are approximately preserved. The resonant states are not members of chaotic bath of short-range states. Similar resonances are expected to be a common feature of alkali-metal diatom + atom systems.

* These authors contributed equally to this work.
† matthew.frye@durham.ac.uk
‡ J.M.Hutson@durham.ac.uk
§ bozhao@ustc.edu.cn
¶ clbai@cas.cn
** pan@ustc.edu.cn

I. INTRODUCTION

Ultracold molecules offer great opportunities to study many areas of physics, including fundamental chemical reaction dynamics [1–5], quantum simulation and computing [6–9], and precision measurements of fundamental constants [10–13]. There has been considerable success in producing ultracold ground-state molecules, either by associating pairs of ultracold atoms [14–24] or by direct laser cooling of molecules [12, 25–29]. Understanding collisions of ultracold molecules with themselves and ultracold atoms is now essential to allow control and further cooling of these molecules [30–33] to form the dense stable gases needed for many applications. Further, at such low temperatures, the molecular collisions are highly quantum mechanical in nature, and are thus of fundamental interest in their own right and a powerful tool to unravel the nature of molecular interactions.

Magnetic Feshbach resonances are one of the most important features of ultracold collisions [34]. They occur when the energy of a (quasi-)bound state is tuned across the incoming collision threshold by an external magnetic field. They have been studied extensively in atomic scattering, where they are used to tune interaction strengths to control collisional cooling, study degenerate quantum gases, and investigate strongly interacting systems, amongst other applications. They are also used to associate pairs of atoms into weakly bound molecules through magnetoassociation [35] and provide highly sensitive probes of atomic interaction potentials.

Magnetic Feshbach resonances in collisions involving molecules are far more challenging to understand. Full scattering calculations are hampered by the need for huge basis sets and pathological dependence on uncertainties in the interaction potential [36]. Mayle et al. [37, 38] suggested that the combination of deep anisotropic potentials and large masses produce a dense forest of chaotic short-range states that dominate the scattering properties and cause large collisional sticking times. This idea has been influential, and there is significant experimental evidence for such effects in molecule+molecule scattering [39–41]. However, the densities of states are now expected to be much lower than the original predictions [42], and are also substantially lower for atom+molecule than for molecule+molecule complexes. There is great interest [43] in whether atom+molecule scattering is dominated by such chaotic states, or whether the important features are caused by long-range bound states akin to those involved in atom+atom magnetic Feshbach resonances. Recently, magnetic Feshbach resonances have been observed in collisions of ^{23}Na^{40}K with ^{40}K [23]; however, only a few resonances were observed, so it was not possible to determine the nature of the resonant states or assign quantum numbers to them.

In this paper, we extend the experimental work of Yang et al. [23] and carry out a theoretical study of the resonances. We perform extensive measurements of the Feshbach resonances in 25 collision channels in the magnetic field range between 16 G and 120 G; more than 80 new atom-molecule Feshbach resonances are observed. We use this large set of results to show that the resonances cluster into groups with clear patterns. We assign both spin and rovibrational character to the bound states responsible for the resonances, and conclude that they are relatively simple long-range states and not chaotic short-range states.

II. OBSERVATION OF THE ATOM-MOLECULE FESHBACH RESONANCES

The atom-molecule Feshbach resonances are detected by observing the loss of molecules from an ultracold atom-molecule mixture as a function of magnetic field. The experimental procedures are similar to those in [23]. We first prepare a two-species dark-spot magneto-optical trap of ^{23}Na and ^{40}K atoms and load the atoms into a clover-leaf magnetic trap to perform forced evaporative cooling. The atoms are then loaded into a crossed-beam optical dipole trap (λ=1064 nm) to perform further evaporative cooling. We typically create about 3×10^5 Na atoms and 1.6×10^5 K atoms at a temperature of about 500 nK.

We create weakly bound Feshbach molecules from this atomic mixture by two-photon Raman photoassociation. The technical details are given in our previous work [23]. We use 3 different target Feshbach states and magnetic fields, each associated with an atomic Feshbach resonance [44], depending on the desired hyperfine level of the molecule. The atoms are prepared in an initial state different from the one which shows the Feshbach resonance and coupled to the Feshbach state by blue-detuned Raman light fields. For transitions involving changing the ^{40}K (^{23}Na) state, the single-photon detuning is about $2\pi \times 250$ GHz ($2\pi \times 252$ GHz) relative to the D2 transition of ^{40}K (^{23}Na) atoms, and the Rabi frequency for the corresponding m_f-changing atomic transitions are about $2\pi \times 50$ kHz ($2\pi \times 33$ kHz). Details of the states and resonances involved are given in Table I.

We transfer the molecules from the Feshbach state to a desired hyperfine level of the rovibronic ground state by stimulated Raman adiabatic passage (STIRAP). The ^{23}Na^{40}K molecule in its rovibrational ground state has 36 hyperfine states due to the nuclear spins $i_{\rm Na} = 3/2$ and $i_{\rm K} = 4$. In the free molecule these are coupled only weakly, so at the magnetic field of the experiment they are decoupled with well conserved projections $m_{\rm Na}$ and $m_{\rm K}$, respectively; we therefore label molecular states $(m_{\rm Na}, m_{\rm K})_{\rm mol}$. In this work, 9 different hyperfine levels are prepared. The hyperfine states $(3/2, -4)_{\rm mol}$, $(1/2, -4)_{\rm mol}$, $(-3/2, -3)_{\rm mol}$, $(-1/2, -4)_{\rm mol}$ are created at about 85 G; the first of these

is the absolute ground state. Molecule loss in the atom+molecule mixture is measured in the magnetic field range between 16 G and 106 G in steps of about 0.5 G. The hyperfine states $(-1/2,-3)_{\rm mol}$, $(-1/2,-2)_{\rm mol}$, $(-3/2,-2)_{\rm mol}$, $(-3/2,-1)_{\rm mol}$, and $(-3/2,-4)_{\rm mol}$ are prepared at about 102 G. The magnetic field range studied is between 16 G and 120 G. The intermediate states used in the STIRAP are the hyperfine levels of a mixed rovibronic state formed from $B^1\Pi\ |v=12,J=1\rangle$ and $c^3\Sigma\ |v=35,J=1\rangle$ [45]. These hyperfine levels can be labelled by the quantum numbers $F_1 = i_{\rm Na} + J$ and $F = F_1 + i_{\rm K}$. The hyperfine interaction between the nuclear spin of K atoms and the electron spin is small, and the quantum numbers F_1, m_{F_1}, and $m_F = m_{F_1} + m_{i_{\rm K}}$ are approximately good quantum numbers. The intermediate states used to prepare different hyperfine levels of the ground states are listed in Table I.

TABLE I. The atomic Feshbach resonances used, the hyperfine levels of the intermediate states, and the polarization of the STIRAP lasers required to prepare the molecule in the desired hyperfine level of the rovibronic ground state. The quantum numbers are defined in the main text. The atom-atom resonance at 104 G for $(1,0)_{\rm Na}+(9/2,-9/2)_{\rm K}$ has not been reported before, and its location has been determined by measuring the binding energy of the Feshbach molecules.

Initial state	Feshbach resonance	Hyperfine level of ground state	Intermediate state				Laser polarization	
			F_1	m_{F_1}	$m_{i_{\rm K}}$	m_F	Stokes	pump
$(1,1)_{\rm Na}+(9/2,-5/2)_{\rm K}$	$(1,1)_{\rm Na}+(9/2,-7/2)_{\rm K}$ at 110 G	$(-1/2,-2)_{\rm mol}$	1/2	−1/2	−2	−5/2	π	π
		$(-1/2,-3)_{\rm mol}$	1/2	−1/2	−3	−7/2	π	σ^-
		$(-3/2,-1)_{\rm mol}$	3/2	−3/2	−1	−5/2	π	π
		$(-3/2,-2)_{\rm mol}$	3/2	−3/2	−2	−7/2	π	σ^-
$(1,1)_{\rm Na}+(9/2,-7/2)_{\rm K}$	$(1,1)_{\rm Na}+(9/2,-9/2)_{\rm K}$ at 85 G	$(3/2,-4)_{\rm mol}$	5/2	3/2	−4	−5/2	π	σ^+
		$(1/2,-4)_{\rm mol}$	5/2	1/2	−4	−7/2	π	π
		$(-1/2,-4)_{\rm mol}$	1/2	−1/2	−4	−9/2	π	σ^-
		$(-3/2,-3)_{\rm mol}$	3/2	−3/2	−3	−9/2	π	σ^-
$(1,1)_{\rm Na}+(9/2,-9/2)_{\rm K}$	$(1,0)_{\rm Na}+(9/2,-9/2)_{\rm K}$ at 104 G	$(-3/2,-4)_{\rm mol}$	3/2	−3/2	−4	−11/2	π	σ^-

In the experiment, the pump laser coupling the Feshbach state and the intermediate state is a 805 nm TA-Pro laser, and the Stokes laser coupling the ground state and the intermediate state is a 567 nm TA-SHG laser. The two lasers are locked to a ULE cavity to suppress the noises. The Stokes light is π polarized and the required polarization of the pump light is π, σ^+ or σ^-. Due to the limited optical access, the two lasers propagate perpendicular to the magnetic field. The π polarization is achieved by setting the polarization of the lasers parallel to the magnetic field. The σ polarization is applied by setting the polarization of the pump laser to $\sigma^+ + \sigma^-$ linear polarization. A detailed theoretical analysis of the coupling strength between the Feshbach states and the hyperfine levels of the intermediate states is given in Ref. 46. There are many possible pathways for STIRAP and in principle many hyperfine levels of the rovibronic ground state can be populated. We have chosen hyperfine levels of the excited states so that the desired pathway dominates over the others and the target hyperfine level is prepared. The purity of the hyperfine states of the ground-state molecule is checked by observing that the molecule number after a round-trip STIRAP does not oscillate as a function of the hold time [47].

The ^{40}K atom has electron spin $s = 1/2$ in addition to nuclear spin $i_{\rm K} = 4$; these couple strongly to form $f = 9/2$ and 7/2 at zero field, with projection m_f. At the fields of the experiment, f is a nearly good quantum number and we label the atomic states of ^{40}K by $(f, m_f)_{\rm at}$. The atoms are prepared in the states $(9/2,-9/2)_{\rm at}$, $(9/2,-7/2)_{\rm at}$, and $(9/2,-5/2)_{\rm at}$.

After the atom-molecule mixture is prepared, we ramp the magnetic field to the desired value in a few milliseconds and then hold the atom-molecule mixture for about 7 ms. We program the profile of current of the coil to compensate the residual magnetic field caused by the eddy currents, so that the magnetic field can reach the desired value in about 4 to 6 ms. During the hold time, the magnetic field drifts and fluctuates, and the magnitude of the uncertainty of the magnetic field is proportional to the magnetic field range we ramp. When the magnetic field is ramped from about 102 G to about 16 G, the uncertainty of the magnetic field during the hold time is about 800 mG. The hold time of the atom-molecule mixture is controlled by removing the ^{40}K atoms using resonant light pulses. After that, the magnetic field is ramped back to the initial value in 3 ms. After about 20 ms when the magnetic field is stable, we transfer the ground-state molecules to the Feshbach state by reverse STIRAP. The Feshbach molecules are either directly detected by the standard time-of-flight absorption imaging or are dissociated into free atoms, which are then detected by absorption imaging. During the hold time, molecules are lost from the trap due to inelastic 2-body atom-molecule collisions or 3-body recombination. At resonance, both these loss processes are enhanced and we see characteristic dips in the remaining molecule number as a function of field. We identify these loss features as the atom-molecule Feshbach resonances. Narrow resonances in the low-field region are challenging to detect in the current experiment, both because the long field ramp to the target field creates uncertainties in the final field, and because the signal-to-noise ratio is reduced if molecules are lost in traversing higher-field resonances on the way.

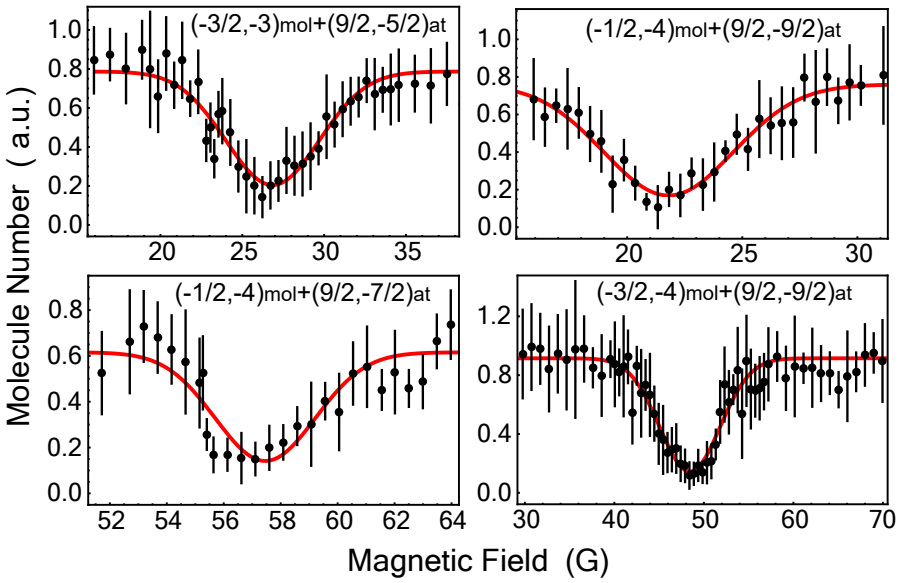


FIG. 1. Example loss features for different collision channels. The remaining molecule numbers are shown as a function of the magnetic field. The solid lines are the fitted Gaussian functions. Error bars represent the standard deviation.

We have searched for Feshbach resonances in 25 of the 27 possible combinations of these 9 molecular states and 3 atomic states. For the combinations $(-3/2,-4)_{\rm mol}+(9/2,-5/2)_{\rm at}$ and $(-1/2,-3)_{\rm mol}+(9/2,-5/2)_{\rm at}$, the background loss rates are very large and our method is not applicable. The resonances for $(-3/2,-2)_{\rm mol}$ at magnetic fields between 43 G and 120 G were studied in our previous work [23], but here we extend the magnetic field range down to 16 G. In total, we observe 84 new atom-molecule Feshbach resonances. Example loss features are shown in Fig. S6. The other 80 loss features are displayed in the supplementary material. We fit the loss features with Gaussian functions to extract a position B_0 and width δ. Note that the observed width of the loss feature δ is not the same quantity as the theoretical width Δ that describes the pole in scattering length associated with the resonance. We give results for all resonances observed in Tables II and III, for the low- and high-field groups of resonances, respectively.

III. ASSIGNMENT OF THE LOW-FIELD ATOM-MOLECULE FESHBACH RESONANCES

In order to interpret these resonances, we need to describe the resonant bound states that cause them and assign their quantum numbers $X^{\rm res}$. We look for explanations in terms of resonances of as few different characters as possible; here the character is defined by the rovibrational state of the triatomic complex and the changes $\Delta X = X^{\rm res} - X^{\rm in}$ between incoming and resonant states for the remaining quantum numbers. If a resonance of a particular character exists at one threshold, a resonance of that character is expected to exist at every threshold where it is allowed.

In the three-atom complex, the diatom rotation n couples to the angular momentum L of the atom and diatom around one another to form N, which represents the total spin-free angular momentum. The quantum numbers (v, n, L, N), with v the diatom vibrational quantum number, provide a good representation in the long-range region where the interaction potential is weak, except for coupling to spins and the magnetic field. The incoming states relevant to the experiment all have $v^{\rm in} = n^{\rm in} = 0$; since $L^{\rm in} = 0$ dominates at the temperature of the experiment, this implies $N^{\rm in} = 0$. The electronic interaction potential is strong and highly anisotropic at short range, which results in complicated states with strongly mixed n, L, and v, but it does not mix N.

The interaction potential between ground-state NaK and K is strongly anisotropic, but there is only a single Born-Oppenheimer potential-energy surface that correlates with the incoming states. There is thus no strong coupling due to differences between two potentials, as there is in collisions of two alkali-metal atoms, or as there would be in collisions of an electron-spin-doublet molecule with an alkali-metal atom. The important couplings are expected to include various Zeeman, spin-rotation, and hyperfine couplings [48, 49]. A detailed description and estimation of the strength of these couplings is beyond the scope of this paper, but they are expected to be fairly weak and to act essentially perturbatively. This means that the bound states can be usefully labeled with the same spin quantum numbers as the incoming states, even if there is significant coupling of s to the molecular nuclear spins at short range. This situation has some similarities with that in alkali+^{1}S systems [50–54].

TABLE II. Atom-molecule Feshbach resonances in the low-field group, along with the assigned quantum numbers for the bound states that cause them as described in the main text.

Initial State		Measured		Assigned quantum numbers				
m_{Na}	m_{K}	B_0 (G)	δ (G)	m_f	m_{Na}	m_{K}	N	M_N
Initial state of the K atom $(f, m_f) = (9/2, -9/2)$								
$-3/2$	-3	20.9	3.2	$-7/2$	$-3/2$	-4	1 or 2	0
$-3/2$	-2	19.4	2.6	$-7/2$	$-3/2$	-3	1 or 2	0
$-3/2$	-1	19.0	1.0	$-7/2$	$-3/2$	-2	1 or 2	0
$-1/2$	-4	21.8	3.9	$-7/2$	$-3/2$	-4	1 or 2	0
$-1/2$	-3	19.3	5.4	$-7/2$	$-3/2$ or $-1/2$	-3 or -4	1 or 2	0
$-1/2$	-2	19.3	2.9	$-7/2$	$-3/2$ or $-1/2$	-2 or -3	1 or 2	0
$1/2$	-4	16.6	0.7	$-7/2$	$1/2$	-4	1 or 2	-1
$1/2$	-4	20.9	3.9	$-7/2$	$-1/2$	-4	1 or 2	0
$3/2$	-4	17.1	0.9	$-7/2$	$3/2$	-4	1 or 2	-1
$3/2$	-4	20.1	1.7	$-7/2$	$1/2$	-4	1 or 2	0
Initial state of the K atom $(f, m_f) = (9/2, -7/2)$								
$-3/2$	-4	19.6	2.0	$-5/2$	$-3/2$	-4	1 or 2	-1
$-3/2$	-3	22.4	2.8	$-5/2$	$-3/2$	-4	1 or 2	0
$-3/2$	-2	23.6	3.6	$-5/2$	$-3/2$	-3	1 or 2	0
$-3/2$	-1	24.3	2.5	$-5/2$	$-3/2$	-2	1 or 2	0
$-1/2$	-4	23.5	5.2	$-5/2$	$-3/2$	-4	1 or 2	0
$-1/2$	-3	22.9	5.9	$-5/2$	$-3/2$ or $-1/2$	-3 or -4	1 or 2	0
$-1/2$	-2	23.1	4.0	$-5/2$	$-3/2$ or $-1/2$	-2 or -3	1 or 2	0
$1/2$	-4	24.8	5.7	$-5/2$	$-1/2$	-4	1 or 2	0
$3/2$	-4	19.8	0.6	$-5/2$	$3/2$	-4	1 or 2	-1
$3/2$	-4	24.9	1.5	$-5/2$	$1/2$	-4	1 or 2	0
Initial state of the K atom $(f, m_f) = (9/2, -5/2)$								
$-3/2$	-3	26.8	3.9	$-3/2$	$-3/2$	-4	1 or 2	0
$-3/2$	-2	29.7	5.2	$-3/2$	$-3/2$	-3	1 or 2	0
$-3/2$	-1	31.7	1.9	$-3/2$	$-3/2$	-2	1 or 2	0
$-1/2$	-4	26.1	4.9	$-3/2$	$-3/2$	-4	1 or 2	0
$-1/2$	-2	27.2	1.0	$-3/2$	$-3/2$ or $-1/2$	-2 or -3	1 or 2	0
$1/2$	-4	25.1	0.4	$-3/2$	$1/2$	-4	1 or 2	-1
$1/2$	-4	29.7	3.0	$-3/2$	$-1/2$	-4	1 or 2	0
$3/2$	-4	31.2	3.1	$-3/2$	$1/2$	-4	1 or 2	0

We consider first the group of resonances between 16 and 32 G, which we refer to as the low-field group. 28 such resonances are currently observed. The general layout of the resonances in field must come from the atomic quantum numbers (f, m_f), since the associated magnetic moments are far larger than the magnetic moments of the molecule; one or both of f and m_f must change for the resonant state to cross the incoming threshold. The lowest state of ^{40}K is $(9/2, -9/2)_{\mathrm{at}}$ and is fully spin-stretched, so the resonances observed for this incoming state must have $\Delta m_f = +1$. This selection rule can explain resonances for all three atomic states investigated, so it seems likely that this character applies to all resonances in the low-field group.

In order to determine f^{res} for these resonances, we consider what each possibility would imply about the levels. We expect that, towards zero field, sublevels with different ${m_f}^{\mathrm{res}}$ will approach one another to form a single clear group, which may have internal structure due to hyperfine couplings in the triatomic complex. We therefore calculate the implied energy of the resonant state, determining ${m_f}^{\mathrm{res}}$ from $\Delta m_f = +1$ and considering $f^{\mathrm{res}} = 9/2$ or $7/2$. We project each bound state back to zero field, assuming it remains at a constant binding energy below its corresponding threshold; this neglects mixing between different levels in the group, but should be a good first approximation. The results of this are shown in Fig. 2.

The red lines in Fig. 2 show that the pattern of resonances is consistent with a closely spaced group of zero-field bound states with $f^{\mathrm{res}} = 9/2$. These have binding energies centred near 8 MHz and spread across about 5 MHz. Such a closely spaced group is unlikely to occur by coincidence. They produce a tightly bunched group of resonances at each atomic threshold, spread over less than 6 G for each m_f. Conversely, the blue lines for an assignment to $f^{\mathrm{res}} = 7/2$ diverge towards zero field and would imply zero-field binding energies spread across at least 20 MHz. However, in this case the states with a given value of ${m_f}^{\mathrm{res}}$ would be expected to cause additional resonances with $\Delta m_f = 0$ and -1 when they cross the higher thresholds. In fact the number of resonances at higher thresholds is similar to that at the $m_f = -9/2$ threshold. It is thus probable that the low-field resonances arise from states with $f^{\mathrm{res}} = 9/2$.

TABLE III. Atom-molecule Feshbach resonances in the high-field group, along with the assigned quantum numbers for the bound states that cause them as described in the main text.

Initial State		Measured		Assigned quantum number
m_{Na}	m_{K}	B_0 (G)	δ (G)	m_f
Initial state of the K atom $(f, m_f) = (9/2, -9/2)$				
$-3/2$	-4	48.4	4.8	$-7/2$
$-3/2$	-3	47.8	3.0	$-7/2$
$-3/2$	-2	48.5	2.1	$-7/2$
$-3/2$	-2	90.3	2.2	$-7/2$
$-3/2$	-1	50.6	1.1	$-7/2$
$-3/2$	-1	59.6	1.3	$-7/2$
$-3/2$	-1	95.3	1.9	$-7/2$
$-1/2$	-4	43.4	0.6	$-7/2$
$-1/2$	-4	47.7	1.9	$-7/2$
$-1/2$	-3	45.1	0.5	$-7/2$
$-1/2$	-3	48.8	1.7	$-7/2$
$-1/2$	-2	50.5	1.3	$-7/2$
$-1/2$	-2	59.7	3.4	$-7/2$
$-1/2$	-2	94.9	0.6	$-7/2$
$1/2$	-4	43.4	0.4	$-7/2$
$1/2$	-4	45.4	0.4	$-7/2$
$1/2$	-4	48.8	1.1	$-7/2$
$3/2$	-4	81.5	0.3	$-7/2$
$3/2$	-4	83.4	0.3	$-7/2$
Initial state of the K atom $(f, m_f) = (9/2, -7/2)$				
$-3/2$	-4	63.2	12.3	$-5/2$
$-3/2$	-3	52.0	0.5	$-7/2$
$-3/2$	-3	57.6	5.3	$-7/2$
$-3/2$	-3	102.9	3.0	$-7/2$
$-3/2$	-2	54.6	0.6	$-7/2$
$-3/2$	-2	59.4	3.1	$-5/2$
$-3/2$	-2	101.1	0.6	$-7/2$
$-3/2$	-2	106.3	1.7	$-7/2$
$-3/2$	-1	57.7	0.7	$-5/2$
$-3/2$	-1	62.2	2.2	$-5/2$
$-3/2$	-1	106.0	0.7	$-7/2$
$-1/2$	-4	57.5	2.5	$-5/2$
$-1/2$	-3	59.4	2.7	$-5/2$
$-1/2$	-3	68.7	3.7	$-5/2$
$-1/2$	-3	101.0	0.3	$-7/2$
$-1/2$	-3	106.5	1.1	$-7/2$
$-1/2$	-2	62.3	2.2	$-5/2$
$-1/2$	-2	72.1	1.8	$-5/2$
$1/2$	-4	51.8	0.3	$-7/2$
$1/2$	-4	59.2	0.9	$-5/2$
Initial state of the K atom $(f, m_f) = (9/2, -5/2)$				
$-3/2$	-3	57.8	3.6	$-7/2$
$-3/2$	-3	63.1	1.2	$-5/2$
$-3/2$	-3	70.0	2.4	$-5/2$
$-3/2$	-3	102.4	2.0	$-7/2$
$-3/2$	-2	68.2	1.0	$-5/2$
$-3/2$	-2	74.5	3.7	$-5/2$
$-3/2$	-2	83.5	1.6	$-3/2$
$-3/2$	-1	72.9	1.2	$-5/2$
$-3/2$	-1	79.3	2.3	$-3/2$
$-3/2$	-1	87.2	0.7	$-3/2$
$-3/2$	-1	90.1	1.2	$-3/2$
$-1/2$	-4	56.8	4.0	$-7/2$
$-1/2$	-4	62.6	1.0	$-5/2$
$-1/2$	-4	69.5	1.3	$-5/2$
$-1/2$	-4	78.8	2.0	$-3/2$
$-1/2$	-4	100.9	2.1	$-7/2$
$-1/2$	-2	55.9	2.1	$-7/2$
$-1/2$	-2	79.5	2.3	$-3/2$
$-1/2$	-2	83.3	0.8	$-3/2$
$-1/2$	-2	90.4	1.9	$-3/2$
$1/2$	-4	51.7	3.2	$-7/2$
$1/2$	-4	63.7	0.3	$-5/2$
$1/2$	-4	73.7	0.8	$-5/2$
$1/2$	-4	77.7	0.4	$-3/2$
$1/2$	-4	83.7	1.2	$-3/2$
$3/2$	-4	50.5	0.3	$-7/2$
$3/2$	-4	56.2	1.4	$-7/2$

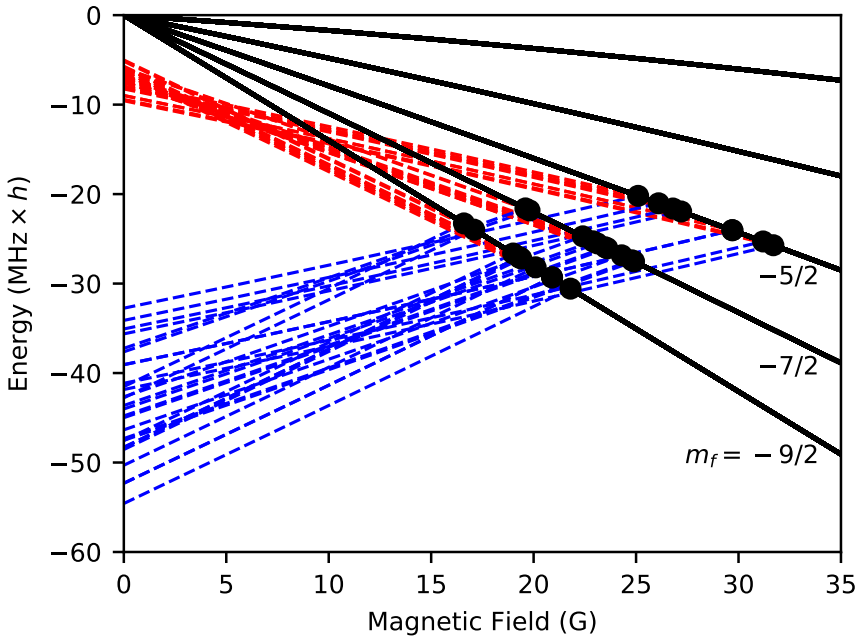


FIG. 2. Observed positions of resonances in the low-field group (black dots), with projections back to zero field assuming $f^{\rm res} = 9/2, \Delta m_f = +1$ (red dashed lines) and $f^{\rm res} = 7/2, \Delta m_f = +1$ (blue dashed lines). Black solid lines indicate thresholds. The weak Zeeman effect of the molecular spins is neglected.

To assign any further quantum numbers, we must look at the detailed patterns of resonances. The low-field resonances are sometimes observed in pairs at the same threshold, so there must be (at least) two characters of resonances in this group. For the thresholds where both resonances are observed, there is a consistent pattern that the one at higher field is wider than the one at lower field, and we label these as having characters A and B respectively. For thresholds where there is only one resonance observed, it is possible that one of the resonances is systematically missing due to selection rules, but it is also possible that the second resonance may be present but not observed.

There is one resonance observed for the incoming combination $(-3/2,-4)_{\rm mol}+(9/2,-7/2)_{\rm at}$, for which the molecule is in its spin-stretched state. This resonance must have $\Delta m_{\rm mol} = \Delta m_{\rm Na} + \Delta m_{\rm K} \geq 0$. Combined with $\Delta m_f = +1$, as discussed above, and conservation of total projection, $\Delta M_{\rm tot} = \Delta m_{\rm mol} + \Delta m_f + \Delta M_N = 0$, this implies that $\Delta M_N \leq -1$ and so $N^{\rm res} \neq 0$. States with different $N^{\rm res}$ are expected to be far apart in energy, so all states in this group must have the same value of $N^{\rm res}$, but may have different ${M_N}^{\rm res}$. There are no terms in the fine, hyperfine or Zeeman Hamiltonian that can directly change N by more than 2, and only the small nuclear electric quadrupole interaction has $\Delta M_N > 1$ [49]; the most likely interpretation is therefore that $N^{\rm res} = 1$ or 2, and that the two characters of resonances in the low-field group are $(\Delta M_N, \Delta m_{\rm mol}) = (-1,0)$ and $(0,-1)$. The latter is missing at the threshold $(-3/2,-4)_{\rm mol} + (9/2,-7/2)_{\rm at}$ because the molecule is spin-stretched, so the observed resonance must have character $(-1,0)$. However, it is not easily assigned as either A or B from its position and width.

For the incoming combination $(-3/2,-4)_{\rm mol}+(9/2,-9/2)_{\rm at}$, no resonance is observed at all, but we expect one with character $(-1,0)$. This resonance might be missed either because it is outside the region of observation or because it is too narrow. Both of these are more likely if it is of character B, so we tentatively assign character A to be $(0,-1)$ and character B to be $(-1,0)$.

This assignment determines the spin character of the resonant bound states almost completely. The resulting quantum numbers are included in Tables II and III. The only remaining ambiguities are in cases where different values of $\Delta m_{\rm Na}$ and $\Delta m_{\rm K}$ can sum to give the same $\Delta m_{\rm mol}$. This might, for example, lead to additional resonances for collisions involving $(-1/2,-3)_{\rm mol}$, but the present experiments have not resolved any such features.

Our assignment implies that there is a rovibrational state of the triatomic complex with $N^{\rm res} \geq 1$ that lies very close to threshold. If this has $f^{\rm res} = 9/2$, it is bound by less than 10 MHz. For a system with unknown scattering length, an argument based on single-channel quantum defect theory [49, 55] indicates there is a 9% (4%) prior probability of finding a p (d)-wave state within 10 MHz of threshold. The real system is more complex than a single channel, but this estimate is appropriate for a state so close to threshold. Conversely, if the state has $f^{\rm res} = 7/2$, its binding energy must be in a narrow range within 50 MHz of the atomic hyperfine splitting; the corresponding probability for

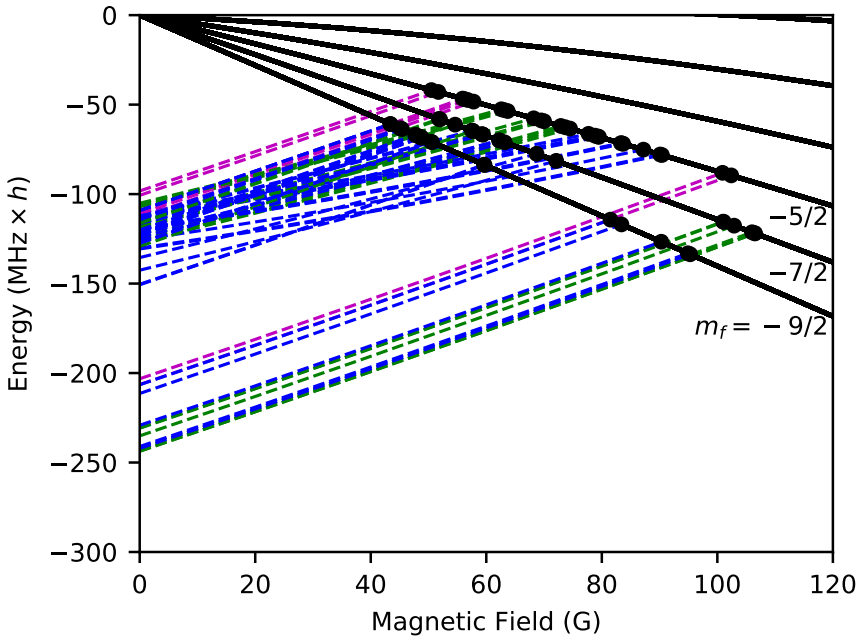


FIG. 3. Observed positions of resonances in the high-field group (black dots), with projections back to zero field assuming $f^{\rm res} = 7/2, \Delta m_f = +1$ (blue dashed lines); $f^{\rm res} = 7/2, \Delta m_f = 0$ (green dashed lines); or $f^{\rm res} = 7/2, \Delta m_f = -1$ (magenta dashed lines). Each resonance is tentatively assigned to one of these options. Black solid lines indicate thresholds. The weak Zeeman effect of the molecular spins is neglected.

this is 2% for either a p-wave or a d-wave state. The final possibility is a state with $n > 0$, for which $N > 0$ is allowed even if $L = 0$. The probability of such a short-range bound state existing in the top 10 MHz of the well is low for any individual value of n and v, but much larger when the full phase space is considered [42]. We estimate the density of states near threshold to be 0.3 GHz^{-1} for NaK+K [48], so there is only about a 0.3% prior probability of finding such a state within 10 MHz of threshold.

The bound state that causes the low-field resonances is therefore most likely a very weakly bound long-range state. Such a bound state will have the character predominantly of the separated atom and molecule in their respective states. This presents a physical picture where the complicated short-range rovibrational couplings are relatively unimportant and the relevant states of the complex are remarkably simple. This is in sharp contrast to the picture of resonances caused by chaotic short-range states, as suggested by Mayle et al. [37].

The long-range nature of the states responsible for the low-field resonances suggests that similar resonances will be present in other alkali-metal atom+diatom systems. For each value of $L^{\rm res}$, there will always be one long-range rovibrational state of the triatomic complex within a certain "bin" of energy below threshold [55]. For low $L^{\rm res}$, such a state is likely to couple to the incoming states to produce a group of magnetically tunable Feshbach resonances below a certain characteristic magnetic field. The depth of the top bin and the corresponding characteristic field depend on the masses of the atom and molecule and on the long-range dispersion coefficient. If $f^{\rm res} = 9/2$, the least-bound state for ^{23}Na^{40}K+^{40}K lies in the upper part of its bin, but for other systems this may not be the case; nevertheless, analogous resonances are typically expected at fields below 400 G for heavier systems [49].

The remaining 66 resonances span from 43 G to 107 G. We will refer to these as the high-field group. They do not form so coherent a pattern as the low-field group, and may arise from sets of resonances with several different characters. In the same way as for the low-field group, the resonances at thresholds with ${m_f}^{\rm in} = -9/2$ must have $\Delta m_f = +1$. However, at thresholds with ${m_f}^{\rm in} = -7/2$ there are a larger number of resonances than for ${m_f}^{\rm in} = -9/2$. This increase is probably caused by resonances with $\Delta m_f = 0$, which are allowed at thresholds with ${m_f}^{\rm in} \geq -7/2$. The further increase in the number of resonances at thresholds with ${m_f}^{\rm in} = -5/2$ can similarly be attributed to $\Delta m_f = -1$. As discussed above, at least one of f or m_f must change between the incoming and bound states, so $\Delta m_f = 0$ implies $\Delta f \neq 0$. We thus conclude that the high-field resonances probably arise from resonant states with $f^{\rm res} = 7/2$.

We project the bound states for this group of resonances back to zero field as described above. We take $f^{\rm res} = 7/2$ for all resonances in this group, but ${m_f}^{\rm res}$ is not unambiguously assigned for ${m_f}^{\rm in} \geq -7/2$, so we pick values that

produce as simple a pattern as possible. The implied bound-state pattern is shown in Fig. 3. Many of the states appear to converge towards a zero-field grouping between −105 and −130 MHz, relative to the $f^{\rm in} = 9/2$ thresholds, with a few surrounding outliers. This is not intended to provide a definitive assignment for individual states, but to indicate that a plausible interpretation along these lines may be possible. The zero-field states between −200 and −250 MHz seem to form a separate group, but there are too few of them to identify clear patterns.

The character of the states responsible for the high-field resonances remains uncertain, but there are a few likely possibilities. They might arise from states with $v^{\rm res} = n^{\rm res} = 0$, bound by just the 1.3 GHz of the atomic hyperfine splitting; they might arise from a low-lying excited rotational state with $n^{\rm res} > 0$, bound by the rotational excitation energy $bn(n+1)$ where $b/h = 2.9$ GHz, either with or without atomic hyperfine excitation; or they might arise from a complicated short-range state of the kind suggested by Mayle et al. [37]. The first of these possibilities would still have substantial long-range character, with decreasing amounts for the subsequent possibilities.

IV. CONCLUSION

In summary, we have performed a detailed experimental and theoretical study of the ultracold atom-molecule Feshbach resonances between ^{23}Na^{40}K and ^{40}K. More than 80 new Feshbach resonances have been observed for a range of initial states. We have presented a detailed theoretical interpretation of the low-field group of resonances and assigned quantum numbers to the bound states that cause them. This allows us to determine the nature of the resonant states: they are likely to be remarkably simple long-range states with the character of the separated atom and molecule. Such states are very different from the chaotic short-range states proposed by Mayle et al. [37]. The simplicity of the long-range states allows understanding and offers the possibility of controlling collisions using these resonances. We expect similar resonances to be observable in other alkali-metal atom + diatom systems.

ACKNOWLEDGMENTS

This work was supported by the National Key R&D Program of China (under Grant No. 2018YFA0306502), the National Natural Science Foundation of China (under Grant No. 11521063, 11904355), the Chinese Academy of Sciences, the Anhui Initiative in Quantum Information Technologies, Shanghai Municipal Science and Technology Major Project (Grant No.2019SHZDZX01), Shanghai Rising-Star Program (Grant No. 20QA1410000). This work was supported by the U.K. Engineering and Physical Sciences Research Council (EPSRC) Grant No. EP/P01058X/1.

X.-Y. Wang led the experimental work, and Matthew D. Frye led the theoretical work.

DATA AVAILABILITY STATEMENT

All data that support the findings of this study are included within the article (and any supplementary information files).

[1] N. Balakrishnan and A. Dalgarno. "Chemistry at ultracold temperatures." Chem. Phys. Lett., **341**, 652 (2001).
[2] T. V. Tscherbul and R. V. Krems. "Manipulating spin-dependent interactions in rotationally excited cold molecules with electric fields." J. Chem. Phys., **125**, 194311 (2006).
[3] S. Ospelkaus, K.-K. Ni, D. Wang, M. H. G. de Miranda, B. Neyenhuis, G. Quéméner, P. S. Julienne, J. L. Bohn, D. S. Jin, and J. Ye. "Quantum-state controlled chemical reactions of ultracold KRb molecules." Science, **327**, 853 (2010).
[4] J. Rui, H. Yang, L. Liu, D.-C. Zhang, Y.-X. Liu, J. Nan, Y.-A. Chen, B. Zhao, and J.-W. Pan. "Controlled state-to-state atom-exchange reaction in an ultracold atom-dimer mixture." Nature Physics, **13**, 699 (2017).
[5] M.-G. Hu, Y. Liu, D. D. Grimes, Y.-W. Lin, A. H. Gheorghe, R. Vexiau, N. Bouloufa-Maafa, O. Dulieu, T. Rosenband, and K.-K. Ni. "Direct observation of bimolecular reactions of ultracold KRb molecules." Science, **366**, 1111 (2019).
[6] D. DeMille. "Quantum computation with trapped polar molecules." Phys. Rev. Lett., **88**, 067901 (2002).
[7] K.-K. Ni, T. Rosenband, and D. D. Grimes. "Dipolar exchange quantum logic gate with polar molecules." Chem. Sci., **9**, 6830 (2018).
[8] J. A. Blackmore, L. Caldwell, P. D. Gregory, E. M. Bridge, R. Sawant, J. Aldegunde, J. Mur-Petit, D. Jaksch, J. M. Hutson, B. E. Sauer, M. R. Tarbutt, and S. L. Cornish. "Ultracold molecules: a platform for quantum simulation." Quantum Sci. Technol., **4**, 014010 (2019).

[9] R. Sawant, J. A. Blackmore, P. D. Gregory, J. Mur-Petit, D. Jaksch, J. Aldegunde, J. M. Hutson, M. R. Tarbutt, and S. L. Cornish. "Ultracold molecules as qudits." New J. Phys., **22**, 013027 (2020).

[10] M. S. Safronova, D. Budker, D. DeMille, D. F. J. Kimball, A. Derevianko, and C. W. Clark. "Search for new physics with atoms and molecules." Rev. Mod. Phys., **90**, 025008 (2018).

[11] J. Kobayashi, A. Ogino, and S. Inouye. "Measurement of the variation of electron-to-proton mass ratio using ultracold molecules produced from laser-cooled atoms." Nature Comm., **10**, 3771 (2019).

[12] B. L. Augenbraun, Z. D. Lasner, A. Frenett, H. Sawaoka, C. Miller, T. C. Steimle, and J. M. Doyle. "Laser-cooled polyatomic molecules for improved electron electric dipole moment searches." New Journal of Physics, **22**, 022003 (2020).

[13] N. J. Fitch, J. Lim, E. A. Hinds, B. E. Sauer, and M. R. Tarbutt. "Methods for measuring the electron's electric dipole moment using ultracold YbF molecules." Quantum Science and Technology, **6**, 014006 (2020).

[14] K.-K. Ni, S. Ospelkaus, M. H. G. de Miranda, A. Pe'er, B. Neyenhuis, J. J. Zirbel, S. Kotochigova, P. S. Julienne, D. S. Jin, and J. Ye. "A high phase-space-density gas of polar molecules in the rovibrational ground state." Science, **322**, 231 (2008).

[15] F. Lang, K. Winkler, C. Strauss, R. Grimm, and J. Hecker Denschlag. "Ultracold molecules in the rovibrational ground state." Phys. Rev. Lett., **101**, 133005 (2008).

[16] J. G. Danzl, M. J. Mark, E. Haller, M. Gustavsson, R. Hart, J. Aldegunde, J. M. Hutson, and H.-C. Nägerl. "An ultracold, high-density sample of rovibronic ground-state molecules in an optical lattice." Nature Physics, **6**, 265 (2010).

[17] T. Takekoshi, L. Reichsöllner, A. Schindewolf, J. M. Hutson, C. R. Le Sueur, O. Dulieu, F. Ferlaino, R. Grimm, and H.-C. Nägerl. "Ultracold dense samples of dipolar RbCs molecules in the rovibrational and hyperfine ground state." Phys. Rev. Lett., **113**, 205301 (2014).

[18] P. K. Molony, P. D. Gregory, Z. Ji, B. Lu, M. P. Köppinger, C. R. Le Sueur, C. L. Blackley, J. M. Hutson, and S. L. Cornish. "Creation of ultracold $^{87}Rb^{133}Cs$ molecules in the rovibrational ground state." Phys. Rev. Lett., **113**, 255301 (2014).

[19] F. Wang, X. He, X. Li, B. Zhu, J. Chen, and D. Wang. "Formation of ultracold NaRb Feshbach molecules." New J. Phys., **17**, 035003 (2015).

[20] J. W. Park, S. A. Will, and M. W. Zwierlein. "Ultracold dipolar gas of fermionic $^{23}Na^{40}K$ molecules in their absolute ground state." Phys. Rev. Lett., **114**, 205302 (2015).

[21] M. Guo, B. Zhu, B. Lu, X. Ye, F. Wang, R. Vexiau, N. Bouloufa-Maafa, G. Quéméner, O. Dulieu, and D. Wang. "Creation of an ultracold gas of ground-state dipolar $^{23}Na^{87}Rb$ molecules." Phys. Rev. Lett., **116**, 205303 (2016).

[22] F. Seeßelberg, N. Buchheim, Z.-K. Lu, T. Schneider, X.-Y. Luo, E. Tiemann, I. Bloch, and C. Gohle. "Modeling the adiabatic creation of ultracold polar $^{23}Na^{40}K$ molecules." Phys. Rev. A, **97**, 013405 (2018).

[23] H. Yang, D.-C. Zhang, L. Liu, Y.-X. Liu, J. Nan, B. Zhao, and J.-W. Pan. "Observation of magnetically tunable Feshbach resonances in ultracold $^{23}Na^{40}K + {}^{40}K$ collisions." Science, **363**, 261 (2019).

[24] K. K. Voges, P. Gersema, M. Meyer zum Alten Borgloh, T. A. Schulze, T. Hartmann, A. Zenesini, and S. Ospelkaus. "Ultracold gas of bosonic $^{23}Na^{39}K$ ground-state molecules." Phys. Rev. Lett., **125**, 083401 (2020).

[25] J. F. Barry, D. J. McCarron, E. B. Norrgard, M. H. Steinecker, and D. DeMille. "Magneto-optical trapping of a diatomic molecule." Nature, **512**, 286 (2014).

[26] S. Truppe, H. J. Williams, M. Hambach, L. Caldwell, N. J. Fitch, E. A. Hinds, B. E. Sauer, and M. R. Tarbutt. "Molecules cooled below the Doppler limit." Nature Physics, **13**, 1173 (2017).

[27] L. Anderegg, B. L. Augenbraun, Y. Bao, S. Burchesky, L. W. Cheuk, W. Ketterle, and J. M. Doyle. "Laser cooling of optically trapped molecules." Nature Physics, **14**, 890 (2018).

[28] L. Caldwell, J. A. Devlin, H. J. Williams, N. J. Fitch, E. A. Hinds, B. E. Sauer, and M. R. Tarbutt. "Deep laser cooling and efficient magnetic compression of molecules." Phys. Rev. Lett., **123**, 033202 (2019).

[29] S. Ding, Y. Wu, I. A. Finneran, J. J. Burau, and J. Ye. "Sub-doppler cooling and compressed trapping of YO molecules at μK temperatures." Phys. Rev. X, **10**, 021049 (2020).

[30] H. Son, J. J. Park, W. Ketterle, and A. O. Jamison. "Collisional cooling of ultracold molecules." Nature, **580**, 197 (2020).

[31] G. Valtolina, K. Matsuda, W. G. Tobias, J.-R. Li, L. De Marco, and J. Ye. "Dipolar evaporation of reactive molecules to below the Fermi temperature." Nature, **588**, 239 (2020).

[32] K. Matsuda, L. De Marco, J.-R. Li, W. G. Tobias, G. Valtolina, G. Quéméner, and J. Ye. "Resonant collisional shielding of reactive molecules using electric fields." Science, **370**, 1324 (2020).

[33] S. Jurgilas, A. Chakraborty, C. Rich, L. Caldwell, H. Williams, N. Fitch, B. Sauer, M. D. Frye, J. M. Hutson, and M. Tarbutt. "Collisions between ultracold molecules and atoms in a magnetic trap." Phys. Rev. Lett., **126**, 153401 (2021).

[34] C. Chin, R. Grimm, P. S. Julienne, and E. Tiesinga. "Feshbach resonances in ultracold gases." Rev. Mod. Phys., **82**, 1225 (2010).

[35] T. Köhler, K. Góral, and P. S. Julienne. "Production of cold molecules via magnetically tunable Feshbach resonances." Rev. Mod. Phys., **78**, 1311 (2006).

[36] A. O. G. Wallis, E. J. J. Longdon, P. S. Żuchowski, and J. M. Hutson. "The prospects of sympathetic cooling of NH molecules with Li atoms." Eur. Phys. J. D, **65**, 151 (2011).

[37] M. Mayle, B. P. Ruzic, and J. L. Bohn. "Statistical aspects of ultracold resonant scattering." Phys. Rev. A, **85**, 062712 (2012).

[38] M. Mayle, G. Quéméner, B. P. Ruzic, and J. L. Bohn. "Scattering of ultracold molecules in the highly resonant regime." Phys. Rev. A, **87**, 012709 (2013).

[39] P. D. Gregory, M. D. Frye, J. A. Blackmore, E. M. Bridge, R. Sawant, J. M. Hutson, and S. L. Cornish. "Sticky collisions of ultracold RbCs molecules." Nature Comm., **10**, 3104 (2019).

[40] P. D. Gregory, J. A. Blackmore, S. L. Bromley, and S. L. Cornish. "Loss of ultracold $^{87}Rb^{133}Cs$ molecules via optical excitation of long-lived two-body collision complexes." Phys. Rev. Lett., **124**, 163402 (2020).

[41] Y. Liu, M.-G. Hu, M. A. Nichols, D. D. Grimes, T. Karman, H. Guo, and K.-K. Ni. "Photo-excitation of long-lived transient intermediates in ultracold reactions." Nature Physics, **16**, 1132 (2020).

[42] A. Christianen, T. Karman, and G. C. Groenenboom. "A quasiclassical method for calculating the density of states of ultracold collision complexes." Phys. Rev. A, **100**, 032708 (2019).

[43] G. Quéméner and P. S. Julienne. "Ultracold Molecules under Control." Chem. Rev., **112**, 4949 (2012).

[44] J. W. Park, C.-H. Wu, I. Santiago, T. G. Tiecke, S. Will, P. Ahmadi, and M. W. Zwierlein. "Quantum degenerate Bose-Fermi mixture of chemically different atomic species with widely tunable interactions." Phys. Rev. A, **85**, 051602 (2012).

[45] J. W. Park, S. A. Will, and M. W. Zwierlein. "Two-photon pathway to ultracold ground state molecules of $^{23}Na^{40}K$." New Journal of Physics, **17**, 075016 (2015).

[46] Y.-X. Liu and B. Zhao. "Theoretical analysis of the coupling between Feshbach states and hyperfine excited states in the creation of $^{23}Na^{40}K$ molecule." Chin. Phys. B, **29**, 023103 (2020).

[47] L. Liu, D.-C. Zhang, H. Yang, Y.-X. Liu, J. Nan, J. Rui, B. Zhao, and J.-W. Pan. "Observation of interference between resonant and detuned STIRAP in the adiabatic creation of $^{23}Na^{40}K$ molecules." Phys. Rev. Lett., **122**, 253201 (2019).

[48] M. D. Frye and J. M. Hutson. "Complexes formed in collisions between ultracold alkali-metal diatomic molecules and atoms." arXiv preprint arXiv:2109.07435 (2021).

[49] M. D. Frye and J. M. Hutson. "Long-range states of alkali-metal triatomic complexes." (2021). Unpublished work.

[50] P. S. Żuchowski, J. Aldegunde, and J. M. Hutson. "Ultracold RbSr molecules can be formed by magnetoassociation." Phys. Rev. Lett., **105**, 153201 (2010).

[51] D. A. Brue and J. M. Hutson. "Magnetically tunable Feshbach resonances in ultracold Li-Yb mixtures." Phys. Rev. Lett., **108**, 043201 (2012).

[52] D. A. Brue and J. M. Hutson. "Prospects of forming molecules in $^2\Sigma$ states by magnetoassociation of alkali-metal atoms with Yb." Phys. Rev. A, **87**, 052709 (2013).

[53] V. Barbé, A. Ciamei, B. Pasquiou, L. Reichsöllner, F. Schreck, P. S. Żuchowski, and J. M. Hutson. "Observation of Feshbach resonances between alkali and closed-shell atoms." Nature Physics, **14**, 881 (2018).

[54] B. C. Yang, M. D. Frye, A. Guttridge, J. Aldegunde, P. S. Żuchowski, S. L. Cornish, and J. M. Hutson. "Magnetic Feshbach resonances in ultracold collisions between Cs and Yb atoms." Phys. Rev. A, **100**, 022704 (2019).

[55] B. Gao. "Zero-energy bound or quasibound states and their implications for diatomic systems with an asymptotic van der Waals interaction." Phys. Rev. A, **62**, 050702(R) (2000).

SUPPLEMENTARY MATERIALS

In the supplementary material, the loss spectrum for the other 80 resonances between ^{23}Na^{40}K and ^{40}K are shown in the Figs. S1-S6.

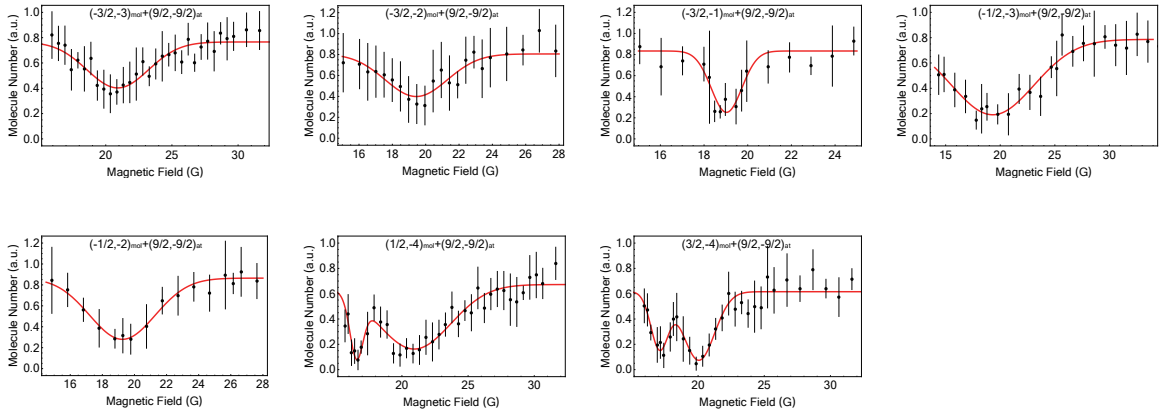


FIG. S1. The low-field resonances with the initial state of the ^{40}K atom in $(9/2, -9/2)$. The remaining molecule numbers are shown as a function of the magnetic field. The solid lines are the fitted Gaussian functions. Error bars represent the standard deviation.

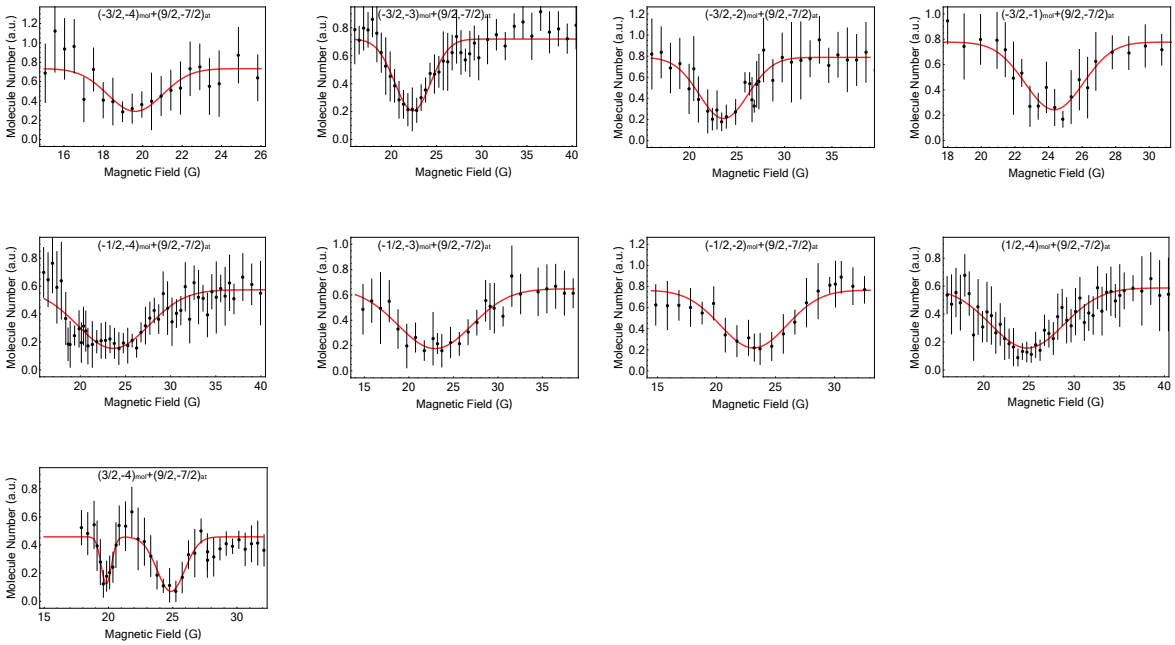


FIG. S2. The low-field resonances with the initial state of the ^{40}K atom in $(9/2, -7/2)$. The remaining molecule numbers are shown as a function of the magnetic field. The solid lines are the fitted Gaussian functions. Error bars represent the standard deviation.

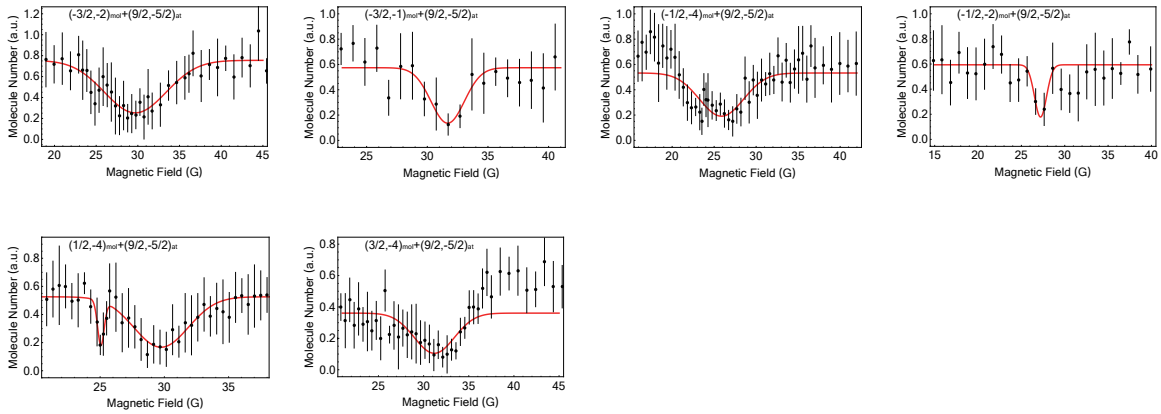


FIG. S3. The low-field resonances with the initial state of the ^{40}K atom in $(9/2, -5/2)$. The remaining molecule numbers are shown as a function of the magnetic field. The solid lines are the fitted Gaussian functions. Error bars represent the standard deviation.

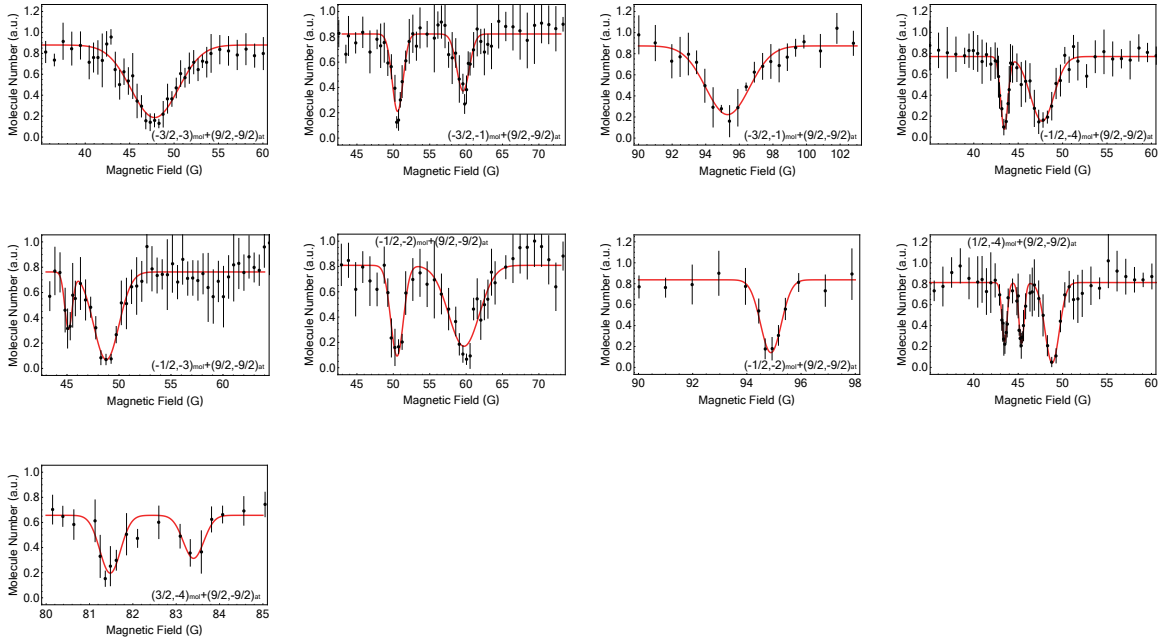


FIG. S4. The high-field resonances with the initial state of the ^{40}K atom in $(9/2, -9/2)$. The remaining molecule numbers are shown as a function of the magnetic field. The solid lines are the fitted Gaussian functions. Error bars represent the standard deviation.

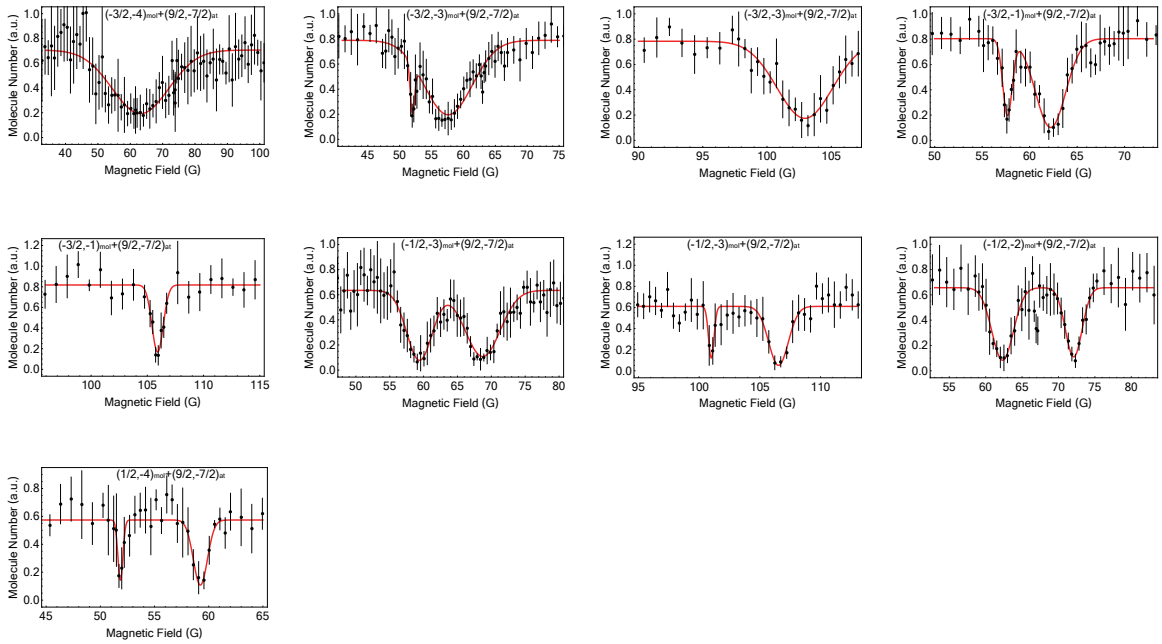


FIG. S5. The high-field resonances with the initial state of the ^{40}K atom in $(9/2, -7/2)$. The remaining molecule numbers are shown as a function of the magnetic field. The solid lines are the fitted Gaussian functions. Error bars represent the standard deviation.

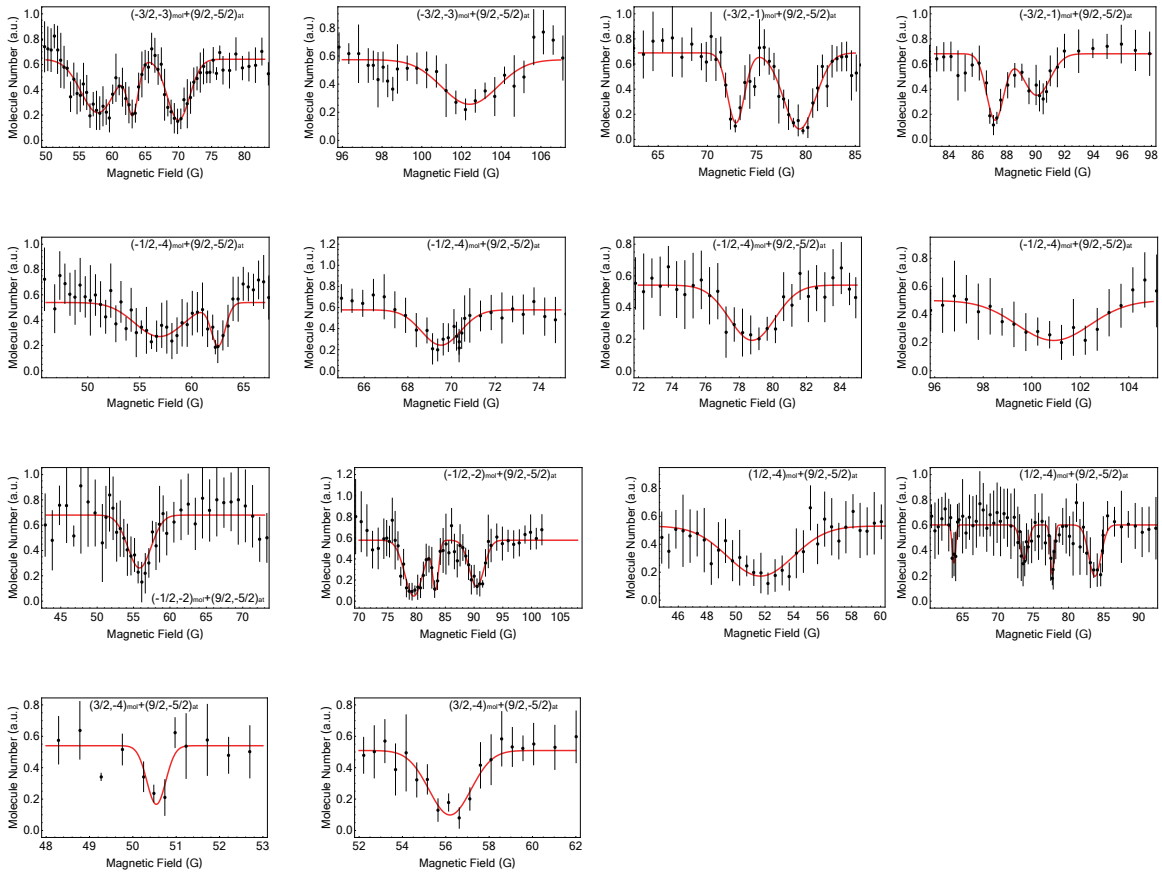


FIG. S6. The high-field resonances with the initial state of the ^{40}K atom in $(9/2, -5/2)$. The remaining molecule numbers are shown as a function of the magnetic field. The solid lines are the fitted Gaussian functions. Error bars represent the standard deviation.